VERSITA

OPTO-ELECTRONICS REVIEW **20**(1), 0–0

DOI: 10.2478/s11772-012-0011-4

Ultrasensitive laser spectroscopy for breath analysis

Invited Paper

J. WOJTAS*[1], Z. BIELECKI[1], T. STACEWICZ[2], J. MIKOŁAJCZYK[1], and M. NOWAKOWSKI[1]

[1]Military University of Technology, 2 Kaliskiego Str., 00-908 Warsaw, Poland
[2]Institute of Experimental Physics, University of Warsaw, 69 Hoża Str., 00-068 Warsaw, Poland

At present there are many reasons for seeking new methods and technologies that aim to develop new and more perfect sensors from different chemical compounds. However, the main reasons are safety ensuring and health care In the paper, recent advances in the human breath analysis by the use of different techniques are presented. We have selected non-invasive ones ensuring detection of pathogenic changes at a molecular level. The presence of certain molecules in the human breath is used as an indicator of a specific disease. Thus, the analysis of the human breath is very useful for health monitoring. We have shown some examples of diseases' biomarkers and various methods capable of detecting them. Described methods have been divided into non-optical and optical methods. The former ones are the following: gas chromatography, flame ionization detection, mass spectrometry, ion mobility spectrometry, proton transfer reaction mass spectrometry, selected ion flow tube mass spectrometry. In recent twenty years, the optical methods have become more popular, especially the laser techniques. They have a great potential for detection and monitoring of the components in the gas phase. These methods are characterized by high sensitivity and good selectivity. The spectroscopic sensors provide the opportunity to detect specific gases and to measure their concentration either in a sampling place or a remote one. Multipass spectroscopy, cavity ring-down spectroscopy, and photo-acoustic spectroscopy were characterised in the paper as well.

Keywords: trace matter detection, breath analysis, diseases biomarkers, absorption spectroscopy, laser spectroscopy, multi-pass spectroscopy, MPS, cavity ring-down spectroscopy, CRDS, cavity enhanced absorption spectroscopy, CEAS, photoacoustic spectroscopy, PAS.

1. Introduction

Serious diseases are the main causes of the worldwide human mortality. In many cases, a proper diagnosis of a disease is delayed and it occurs at the moment when the sickness is incurable. An early diagnostics based on a breath analysis would provide an opportunity for screening which would significantly increase chances for an effective therapy.

At present, the approaches to using the breath analysis for medical diagnostics are the subjects of an intensive investigation around the world. Non-invasive operation (no puncture, no instruments' placing into the body, no contrasts mixtures' application, etc.), easy use (no storage, transport conditions and preparing procedures for analytical samples), ability to re-use, real time measurement, minimum nuisance for patients (especially important for children and the elderly), ability to detect pathogenic changes at the molecular level are the main advantages of these methods. Thus, the analysis of the human breath might be particularly useful for screening diagnostics, treatment in very specific conditions, therapy monitoring, control of exogenous gases (bacterial emissions or poisonous ones) and analysis of metabolic gases.

*e-mail: jwojtas@wat.edu.pl

The gases normally existing in the atmosphere, e.g., N_2, O_2, H_2O, CO_2, appear in a normal human breath in a relatively high concentration (Table 1). Over 1000 various compounds mentioned as "other" have been identified by now.

Table 1. Main components of human breath.

Gas	Percentage	
	Inspired air	Exhaled breath
Nitrogen	78.08	78.00
Oxygen	20.95	16.00
Argon	0.93	1.00
Carbon dioxide	0.04	5.00
Water vapour	1.00–2.00	5.00
Other	0.01	different for each person

The concentration of other specific biomarkers in the human breath depends on the individual characteristics of a person or indicates a symptom of a particular ailment. For example, the concentration of nitric oxide is dependent on age, gender, lung capacity and time of day. For women, such concentration is affected by a phase of menstrual cycle. Moreover, smoking, alcohol consumption, air pollution have also influence on the breath composition (NO level especially, Ref. 1). Typical endogenous trace gases present in breath are listed in Table 2.

Table 2. Endogenous trace gases present in breath (after Ref. 2).

Breath gas	Formula	Typical fraction
Methane	CH_4	2–10 ppm
Carbon monoxide	CO	1–10 ppm
Ammonia	NH_3	0–2 ppm
Acetone	$(CH_3)_2CO$	0–1 ppm
Isoprene	C_5H_8	50–200 ppb
Nitrous oxide	N_2O	50–200 ppb
Nitric oxide	NO	10–50 ppb
Ethane	C_2H_6	0–10 ppb
Pentane	C_5H_{12}	0–10 ppb
Carbonyl sulfide	OCS	0–10 ppb
Hydrogen cyanide	HCN	0–10 ppb

The chemicals caused by physiological factors are also present in the human breath. Their compounds are formed during a manifold of processes: carbon monoxide due to the oxidation of fatty acids, ammonia – as the result of protein catabolism caused by ammonia and amino acids, carbon disulfide is produced by intestinal bacteria, hydrocarbons as a result of metabolism and lipid peroxidation, methanol – due to metabolism of fruit, etc. Examples of these compounds and their typical mixing ratios are listed in Table 3 [3,4].

The presence of certain molecules in the human breath can be used as an indicator (biomarker) of a disease. Examples of biomarkers of some diseases are listed in Table 4. Their early detection is possible by using various trace matter detection methods of high sensitivity. As it was mentioned above, it may have a significant impact on the success of any therapy.

2. Non-optical methods of breath analysis

In order to test biomarkers in exhaled human breath, various methods were developed in the past two decades. At present, the gas chromatography (GC) is the commonest technique used for analysing biomarkers in the exhaled breath. It consists of an injection of the air sample into the chromatographic column where the physic-chemical separation process is carried out [9]. The sample is transported along the column with an inert gas. Chemical compounds of various affinities to the stationary phase move with various speeds. Due to that, the separation of compounds takes place. At the column output, various methods are applied for detection of molecules. These methods include for example: flame ionization detection (FID), mass spectrometry (MS), and ion mobility spectrometry (IMS).

Table 3. Examples of trace gas concentrations in human breath (after Ref. 5).

Gas	Chemical formula	Typical mixing ratio	Physiological source of molecules
Methane	CH_4	2–10 ppm	Gut bacteria
Carbon monoxide	CO	1–10 ppm	Degradation of haemoglobin
Ammonia	NH_3	0–2 ppm	Catabolism of proteins and amino acids
Acetone	$(CH_3)_2CO$	0–1 ppm	Oxidation of fatty acids
Isoprene	C_5H_8	50–200 ppb	Cholesterol synthesis
Nitrous oxide	N_2O	50–200 ppb	Synthesis of enzymes [6,7]
Nitric oxide	NO	10–50 ppb	Production catalysed by NO synthase
Ethane	C_2H_6	0–10 ppb	Lipid peroxidation
Pentane	C_5H_{12}	0–10 ppb	Lipid peroxidation
Carbonyl sulfide	OCS	0–10 ppb	Gut bacteria
Hydrogen cyanide	HCN	0–15 ppb	Pseudomonas aeruginosa

Table 4. Examples of some diseases' biomarkers.

Biomarker	Chemical formula	Disease
Nitric oxide, carbon monoxide	NO, CO	Asthma
Volatile organic compounds	VOCs	Lung cancer
Formaldehyde, pentane	CH_2O, C_5H_{12}	Breast cancer
Acetone	$(CH_3)_2CO$	Diabetes
Ammonia, carbon dioxide	NH_3, CO_2	Stomach ulcers and duodenal ulcers caused by helicobacter pylori
Carbon monoxide	CO	Angina, hyperbilirubinemia
Carbonyl sulphide, ammonia	OCS, NH_3	Liver disease
Carbon disulphide	CS_2	Schizophrenia
Sulphide carbonyl	OCS	Transplant rejection
Hydrogen cyanide	HCN	Cystic fibrosis [8]

In the FID detector, changes of a current resulting from the matter pyrolysis are the main determinants of the detected substances. FID is characterized by high sensitivity, wide range linear response and low level of noise. The detection limit reaches single ppb. For that reason, the FID detector is very often used in breath analysis. The GC-FID sensor has been successfully applied to detect acetone, pentane, isoprene, hexanal and other volatile organic compounds [10] as well as for observation of lung cancer cells and bacterial cultures [11,12].

GC-MS system provides a quantitative analysis of chemical compounds. It is based on determination of mass to charge ratio of ionized atoms or molecules. Its main advantage is high selectivity and sensitivity [13]. The sensitivity of a few ppb has been obtained with this technique for the lung cancer biomarkers detection.

GS-IMS analysers are increasingly applied to the breath analysis contemporarily. Their operating principle is based on a different ions separation while moving in the electric field. Currently available IMS detectors are compact and portable. They provide an opportunity to perform a complex analysis of chemical substances. The determination of trace amounts of aldehydes, ketones, and esters at the level of ppb/ppt is also possible using the GS-IMS analysers.

A separated group of biomarkers detection method is proton transfer reaction mass spectrometry (PTR-MS). A chemical ionization based on a proton transition effect is used. The fact that there is no need to carry out the preliminary procedures of separation of chemical compounds is an important advantage of this method. The instrument is characterized by high sensitivity (below ppt) and high repetition of possible measurements. Therefore, it is an attractive alternative for repeated real-time medical examinations. However, an important limitation of this method is the inability to identify the compounds. Therefore; additional detection methods must be applied. PTR-MS detectors have already been successfully used to analyse isoprene and methanol concentrations which are the potential markers of tumour and inhaled anaesthetics. Moreover, isoprene can be used for a determination of cholesterol in the blood. New opportunities for a non-invasive research of biochemical reactions in the body (e.g. during sleep) can be achieved by using this technique. Such studies were previously impossible especially in the case of the analysis of metabolic processes. Selected ion flow tube mass spectrometry (SIFT-MS) is a dynamically developing technique for breath analysis. In this technique, a chemical ionization of the gas sample is applied. It provides an opportunity for the fast and real-time quantitative analysis of several gases. The sensitivity of ppb level was obtained [14]. That is why the SIFT-MS technique can be effectively used in clinical diagnostics, therapeutic monitoring, and psychological research. Nowadays, thanks to the SIFT-MS technique there are performed: detection of isoprene, acetonitrile, ammonia for cigarette smokers, or methanal for patients with prostate cancer.

Electronic sensors are another group of analysers used to detect biomarkers in the breath [15]. There is a lot of constructions of such sensors, for example bulk acoustic wave sensor, surface acoustic wave sensor [16], sensors with conductive polymers [17], and others [18–20]. So-called electronic noses are important instruments in modern clinical diagnosis. They can be used to detect ammonia, ethanol, NO, CO, etc. The noses are cheap, easy to use and provide quick measurements.

In spite of the fact that many methods of breath analysis are applied, still a lack of these approaches is evident. Each method has its advantages and its limitations. However, at the moment, these approaches cannot be used for common screening with a widely accessible diagnostics due to a big cost of the apparatus and their complicated maintenance. Even the application of electronic sensors, which are the most convenient for the purpose, is limited here by their low sensitivity. Therefore, the search for new methods of breath analysis is strongly motivated. The use of dogs for the detection of diseases' markers in breath confirms the importance of the problem [21].

Optical spectroscopic methods (which are the matter of this paper), especially the laser techniques, have a great potential in the detection and monitoring of the components in the gas phase. These methods are characterized by high sensitivity and good selectivity. The spectroscopic sensors provide opportunity to detect specific gases and to measure their concentration in the place of sampling (so-called *in situ*) or in the distance from the sampling place (so-called *stand-off*). Here, multi-pass spectroscopy (MPS), cavity ring-down spectroscopy (CRDS), and photo-acoustic spectroscopy (PAS) are the most useful. Even though these techniques have been known for decades, their successful application for tracing gas detection has only been possible over the past few years due to the new opportunities arising from the fast development of semiconductor lasers and novel photo-detectors. Due to the tunability of lasers and their narrowband generation, new properties of the optical apparatus occur. The constructions are characterized by low energy consumption, small dimension and weight. They co-operate well with other electronic apparatus (computers) which make their maintenance simple and cheap. That would make possible to install such equipment in ordinary medical offices. All these optical techniques refer to the laser absorption spectrometry.

3. Spectroscopic properties of breath compounds

In a spectrophotometric approach, the absorption is determined by measuring the radiation quenching when passing through the medium (Fig. 1). In such experiment, a decrease in the intensity of radiation which is emitted by a light source (laser) is measured by a photo-receiver. Other approaches consist of measurement of other effects induced by the radiation: temperature changes, acoustic wave detection (OAS), measurement of the electric current or charge in the medium (optogalvanic spectroscopy), etc.

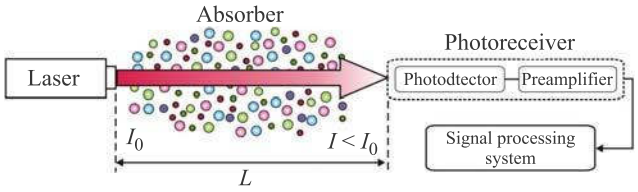

Fig. 1. Idea of absorption method.

Absorption spectrum of a molecule follows various quantum transitions that take place between its energy levels. As an example, the spectrum of NO_2 is shown in Fig. 2.

A short wavelength range (UV) of the absorption spectrum usually corresponds with quantum transitions between the electronic states [22]. These spectra are continuous. Small wavelength scale fluctuations of the cross section within this band reflect the transitions between molecular electro-vibronic levels. At normal conditions when collisional and Doppler broadening takes place, these individual transitions are poorly distinguishable. Therefore the application of UV spectra in a selective detection of species is difficult, especially when the multi-component sample is analysed. Such measurement is usually affected by the interferences due to overlapping of the absorption bands of various molecules.

NO_2 is an exception to this statement. Its electronic absorption band spans from almost 0.3 to 0.5 μm [23]. The range of 0.4–0.46 μm was exploited in several laboratories for sensitive detection (~1 ppb) of this compound in atmosphere [24]. The range corresponds to blue-violet diode lasers [25,26]. It is possible to avoid the interferences due to the fact that normally in the air there is no other compound absorbing in this spectral range.

The absorption bands at the IR wavelengths correspond to transitions between molecular rovibronic levels of the ground electronic state [27,28]. These spectra often consist of series of narrow separated lines (see the example in Fig. 3). Such an absorption band is a good fingerprint of the compound. The careful choice of the absorption lines provides opportunity to selectively detect a certain compound even in the presence of various interferes in a sample.

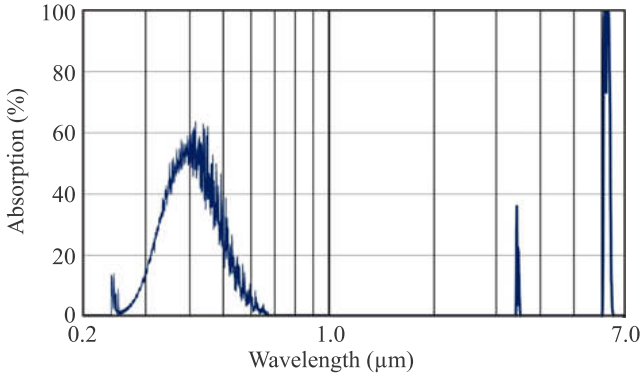

Fig. 2. Absorption spectrum NO_2 in 0.2 to 7 μm range.

In Fig. 3, the procedure of the absorption line selection is presented. It was performed for NO detection. As one can see, H_2O is the main compound which can interfere with the measurement. The wavelength was selected by taking into account the radiation sources available on the market (quantum cascade lasers – QCL) and interferences by water vapour. Therefore for NO, the wavelength of 5.282 μm was chosen [29]. The effective detection also requires the tuning of the laser line to a certain absorption peak with precision of 10^{-5}–10^{-6}.

For heavy molecules, the vibronic absorption spectrum becomes more complicated. When the molecular structure is complicated, due to richness of oscillation mode structure, the spectrum is complex. The absorption lines of various modes overlap and the spectrum is not any good fingerprint of the molecule. One can evaluate that the trace matter detection with the optical methods in multicomponent samples becomes poor when the molecular weight of searched compound is significantly larger than 40 atomic units.

Intensity of radiation registered by a photoreceiver at the wavelength of λ when passing through the absorber (Fig. 1) can be determined using Lambert-Beer law

$$I(\lambda) = I_0(\lambda) \exp[-\alpha(T, \lambda) L], \tag{1}$$

where $I_0(\lambda)$ is the intensity of incident radiation, α denotes the absorption coefficient, while L is the length of the opti-

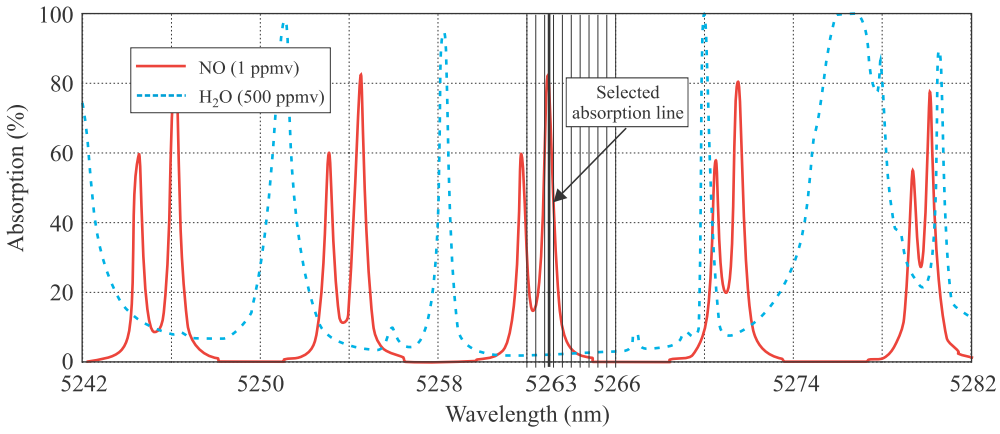

Fig. 3. Selection of absorption line for NO detection.

cal path in the absorber, and T is the temperature of the medium. The value of the absorption coefficient is proportional to the concentration of absorbing molecules N, and the absorption cross section

$$\alpha(T, \lambda) = \sigma(T, \lambda)N. \tag{2}$$

The absorption cross section $\sigma(T, \lambda)$ is the characteristic parameter for a given gas. Its value can be determined in a laboratory, however, for many compounds the parameters of their spectra are available in commercial databases [30, 31]. Here, usually the line strength is given instead of the absorption cross section. The relation between the absorption coefficient and the line strength $S(T)$ is given by

$$\alpha(\lambda, T) = NS(T)g(\lambda - \lambda_0), \tag{3}$$

where $g(\lambda - \lambda_0)$ denotes the normalized line shape

$$\int_0^\infty g(\lambda - \lambda_0)d\lambda = 1, \tag{4}$$

which includes the effects of line broadening due to Doppler and collision phenomena. Therefore

$$\sigma(\lambda, T) = S(T)g(\lambda - \lambda_0). \tag{5}$$

The absorption cross section and the absorption coefficient as well as the line strength depend on the temperature T, which is also related to elastic and non-elastic collision effects. Therefore $S(T)$ is well determined for a certain medium (air usually) as well as its composition (humidity) and pressure.

For breath molecules, the typical absorption cross section values are from $\sigma \sim 10^{-20}$ to $\sim 10^{-18}$ cm^2. As seen in Tables 2 and 3, for the majority of compounds, the detection limit should be better than single ppm ($N \sim 10^{13}$ cm^{-3}). However, for some of them the limit should reach even the level of parts of ppb ($N < 10^{10}$ cm^{-3}). These concentrations are so small that even in the most profitable circumstances the absorption coefficients are: $\alpha = N \cdot \sigma << 10^{-4}$ cm^{-1}. Due to that, the breath analysis cannot be performed with common spectrophotometry which sensitivity is about $\alpha_L \sim 10^{-4}$ cm^{-1}. High sensitivity laser spectroscopy techniques must be applied.

One of these methods is the tuneable diode laser absorption spectroscopy (TDLAS) which operation idea is shown in Fig. 4(a) [32]. Tuneable lasers are used. The laser emission frequency is sinusoidal modulated at about mean frequency of $\bar{\nu}$ according to the formula $\Delta\nu = \bar{\nu} + a\cos(\omega_{\text{mod}} t)$. Thereby the absorption signal is also modulated, and the signal at the detector has the time-dependent form [Fig. 4(b)]. The demodulation of a signal with a lock-in amplifier at twice of modulation frequency ($2\omega_{\text{mod}}$) results in the second derivative of the absorption spectrum, as depicted in Fig. 4(c).

This method offers advantages over conventional spectrophotometry. It provides opportunity to determine the amount of substance fractions of gases from major to trace levels. Compared to other traditional methods used in gas analysis, TDLAS is very selective and fit for *in situ* measurements. The detection limit of 10^{-4}–10^{-6} cm^{-1} is obtained. Higher sensitivity can be obtained by the use of other techniques, like MPS, CRDS, and PAS.

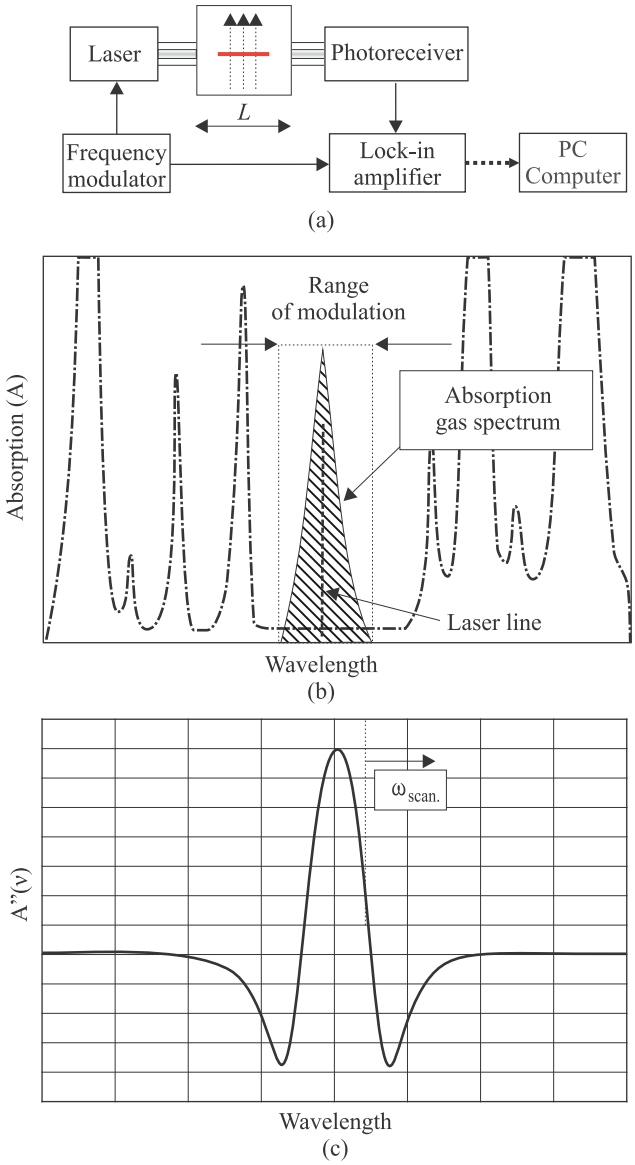

Fig. 4. Operation idea of TDLAS: experimental scheme (a), spectrum scanning (b), and result of measurement (c).

4. Multi-pass cell spectroscopy

The high sensitivity of multi-pass cell spectroscopy (MPS) follows the lengthening of the optical path in the absorber. Its principle is shown in Figs. 5 and 6. The investigated gas sample is contained in a cell composed of two mirrors. The light beam enters the cell through a hole in the mirror and then is reflected many times in the cell. Due to that, its path is much longer than for a single-pass spectroscopy. The sensitivities reaching $\alpha_L \sim 10^{-7}$ cm^{-1} (and even higher) are available. Typical sensitivities available in portable measuring systems are given here. Sensitivities that can be reached in laboratory systems might be much better.

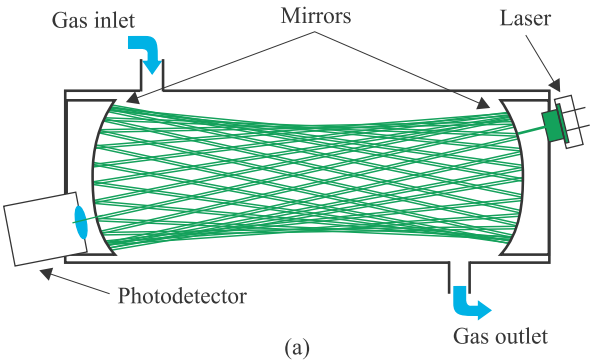

(a)

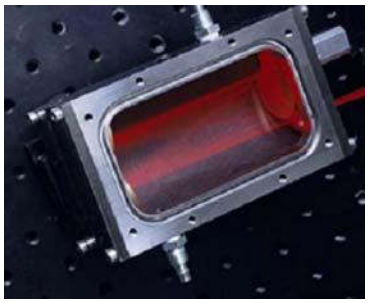

(b)

Fig. 5. Operation idea (a) and photography (b) of White's cell (b) (after Ref. 34).

There are several kinds of this arrangement which differ by a light input and output configuration [33]. In Fig. 5, the principles of increasing the optical path in White cell are shown while the maintenance of Herriott cells is explained in Fig. 6. In White cell, there are two separated holes. One of them is designed for launching the radiation and the other one is used to introduce a light beam while through the other hole the radiation leaves the cell and goes to the detector. In Herriott cell (Fig. 6), the radiation is launched into the cell and it is leaded out to the detector through the same hole.

The optimal application of these methods requires special distribution of the light beams reflected in the cell. The distribution of light spots on the mirrors for White and Herriott approaches is shown in Fig. 7.

5. Cavity ring-down spectroscopy

Cavity ring-down spectroscopy (CRDS) is the most sensitive method of the absorption measurement [35–38]. Its idea is presented in Fig. 8. The radiation pulse I_o is introduced to

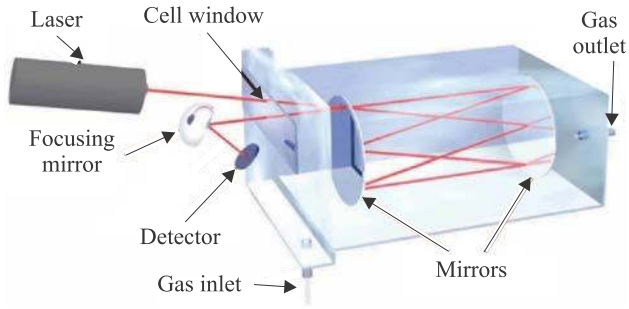

Fig. 6. Application of Herriott's cell.

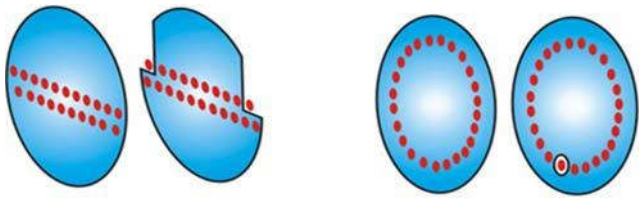

Fig. 7. Mirrors' arrangements in multi-pass White and Herriott cells (dots correspond to light beam spots on the mirrors surfaces).

the optical cavity (resonator) built of mirrors characterized by the very high reflectivity R. Due to multiple reflections between the mirrors, the radiation is trapped in the cavity.

Using Lambert-Beer-Burger law, the changes of the radiation intensity in the cavity can be described by

$$\frac{dI}{dt} = -I_0\left(\frac{c(1-R)}{L} + \alpha c\right). \tag{6}$$

The radiation intensity in the cavity decreases exponentially. The radiation quenching is determined by the registration of radiation leaking trough one of the mirrors

$$I(t) = I_0 e^{-\left\{\frac{[(1-R)+\alpha L]c}{L}\right\}} = I_0 e^{-\frac{t}{\tau_A}}, \tag{7}$$

where I_0 is the initial intensity of light and τ_A is the decay of radiation in the cavity (called cavity ring down time). The decay can be determined from the formula

$$\tau_A = \frac{L}{c[(1-R)+\alpha L]}. \tag{8}$$

For the cavity with no absorber inside ($\alpha = 0$), Eq. (8) can be rewritten as

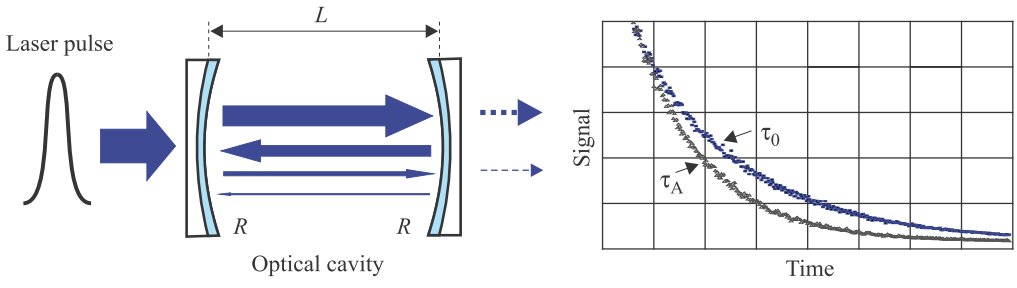

Fig. 8. Idea of CRDS.

$$\tau_0 = \frac{L}{c[(1-R)]}. \tag{9}$$

Comparing the decay times for the resonator filled with an absorber τ_A with that of an empty cavity τ_0 one can find the absorption coefficient and the absorber concentration as well

$$\alpha = N\sigma = \frac{1}{c}\left(\frac{1}{\tau_A} - \frac{1}{\tau_0}\right). \tag{10}$$

The sensitivity of this technique can be better than α_L ~10^{-9} cm^{-1}. In the optical cavity construction, the mirrors of the very high reflectivity R (often exceeding the value of 99.99%) are applied. Due to that, the multiple reflections of a laser beam inside the cavity take place and the effective optical path of the radiation up to several kilometres is achieved. The output signals can be registered with sensitive linear photo-detectors and digital oscilloscopes.

Several modifications of CRDS were developed since the discovery of this technique in 1988. For the breath analysis, the best result might be achieved with continuous wave single mode lasers. The lasers can be precisely tuned in to a narrowband absorption spectrum. It is especially important for the sensitive detection of molecules at their rovibronic transitions – as it was pointed out above (Sect. 3). Its technique so-called CW-CRDS was used for gas detection only in 1997 [39,40]. The diagram of the setup is shown in Fig. 9. The use of CW lasers was possible due to an optical modulator of the laser beam. With this method, a sensitivity of an absorption coefficient registration reaching even value of 10^{-14} cm^{-1} was demonstrated [41].

The operation with single mode lasers, which are tuned in to narrowband absorption resonances, provides problems for the conventional CRDS technique. An optical cavity can effectively store the radiation only if it is precisely tuned in to the cavity modes. Matching the cavity mode with the laser frequency (and with the absorption line as well) requires a control of position of one mirror with a piezoelectric element involved in a feedback loop with an output light intensity detector. That condition strongly complicates the system construction and often causes its instability. The modification of the CRDS technique presented in 1998 [42] provides opportunity to avoid such complication. It is based on an off-axis arrangement of the resonator (Fig. 10). Such solutions are applied in integrated cavity output spectroscopy (ICOS) technique and cavity enhanced absorption spectroscopy (CEAS) technique [43].

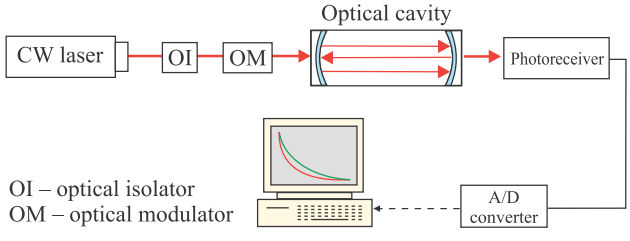

Fig. 9. Scheme of CW-CRDS' setup.

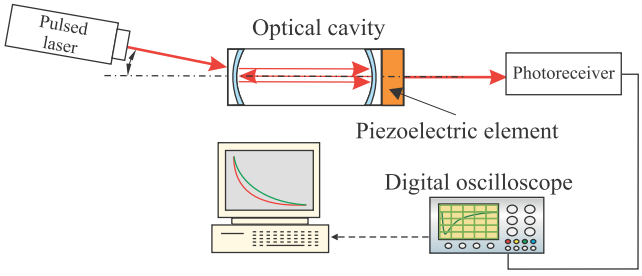

Fig. 10. Idea of CEAS method. In some arrangements, output mirror is moved with piezoelectric element which additionally prevents establishing of cavity mode structure.

In this configuration, the light is repeatedly reflected by the mirrors, however, the reflection points are spatially separated [44]. The free-spectral range (FSR) of an off-axis cavity can be n times less than the FSR of an on-axis aligned cavity, where n is the number of the return trips for which a laser beam returns exactly to its entrance point. Due to that, either the dense mode structure of low finesse occurs or the mode structure is not established at all. Avoiding light interference allows us to eliminate sharp resonances of the cavity, so the problem with laser modes and narrow absorption lines matching does not occur.

The off-axis design eliminates also optical feedback from the cavity to the light source. This is especially important when diode lasers are applied. Moreover, in these configurations the light is many times reflected by the mirrors and it fills out the whole volume of the cavity. In comparison with the ordinary CDRS, the off-axis cavity adjusting is much less sensitive to the cavity misalignment caused, e.g., by the refractive index fluctuations due to turbulences or small mechanical instabilities.

The technique with an intensity modulation of laser radiation (with frequency f) is very useful for the phase shifted CRDS measurement which is characterized by a good precision [45]. The phase shift of a cavity output signal in respect to the laser signal occurs due to the radiation energy storage in the resonator. This shift is expressed by the formula $tg(\varphi) = 4\pi f\tau$. The phase shift measurement for the empty cavity (φ_0) and the cavity filled with the absorber (φ_A) provides the opportunity to calculate the absorption coefficient using Eq. (10)

$$\alpha = \frac{4\pi f}{c}[ctg(\varphi_A) - ctg(\varphi_0)]. \tag{11}$$

While analyzing Eqs. (2) and (8–11) one can find that the threshold concentration which can be found with CRDS methods is

$$N_{GR} = \frac{\Delta\tau}{c\sigma\tau_0^2} = \frac{(1-R)}{\sigma L}\frac{\Delta\tau}{\tau_0} = \frac{(1-R)}{\sigma L}\frac{\Delta\varphi}{tg(\varphi_0)}, \tag{12}$$

where $\Delta\tau$ and $\Delta\varphi$ denote the uncertainty of decay time and phase shift determination, respectively. A high sensitivity of the detection method can be achieved by the use of mirrors of high reflectivity, as well as by lengthening of the cavity

and searching of the absorption resonance of a high cross section. However, the precise measurement of τ and φ (respectively) is also important. As far as the usual precision of $\Delta\tau$ determination is about 1%, the phase shift might be achieved with the precision of about one order of magnitude better especially when a lock-in amplifier is used for this purpose. Moreover, the lock-in amplifier application provides opportunity of simpler interfacing of the apparatus with a computer.

In Fig. 11, the detection system developed by Tittel's research group is given as an example [46,47]. It is prepared for a NO monitoring. Three main subsystems can be distinguished: optical components with the laser and the cavity, the laser driver, and the signal processing unit. In the setup, a quantum cascade laser (QCL) operating at room temperature was applied. The QC lasers are characterized by narrow emission lines and high power. They can be tuned by either driving current or operation temperature. Therefore, the laser is placed in a special housing which controls its temperature. The tuning modulation is made by a special saw-tooth generator. The laser wavelength is controlled by an etalon filled with nitric oxide. The radiation is directed to this etalon. Next, an optical signal at the etalon output is registered with a MCT photodetector. The system provides opportunity to control the laser tuning to the individual NO absorption lines. While removing the mirror, the laser radiation is directed at a small angle to the optical cavity axis. A high density structure of the modes is achieved. It can be additionally destabilized by a modulation of the cavity length with the piezoelectric modulator. The optical signal from the cavity is recorded with a MCT photodiode equipped with a low noise preamplifier. The signal is measured by using a lock-in amplifier which narrowband frequency filter is tuned to the second harmonic of a modulating signal. The determination of a NO concentration is made by using specialized computer software. The measuring procedure, so-called, integrated cavity output spectroscopy (ICOS) is based on a comparison of the signal amplitudes at the input and the output of the cavity [48,49]. For off-axis illumination of the resonator, the wavelength and the electric-field phase information can be neglected leading to a simplified description of the output intensity

$$I = -I_{in}\frac{(1-R)^2\, e^{-\alpha L}}{2\ln(\mathrm{Re}^{-\alpha L})}. \tag{13}$$

When the resonator is "spoiled", the single pass output intensity is calculated from

$$I' = I_{in}(1-R)^2\, e^{-\alpha L}. \tag{14}$$

Due to the energy storage in the cavity, the output intensity is larger than the intensity I' corresponding to a situation when the radiation is not trapped in the resonator. One can show that for ICOS method

$$\alpha = \frac{\ln(R)}{L}\frac{I-I'}{I}. \tag{15}$$

The disadvantage of this method consists in the fact that the precise information about mirror reflectivity is required.

The methods mentioned in this chapter relate to the pulsed or modulated CW laser radiation. The cavity leak-out spectroscopy (CALOS) is a CW variant of CRDS [50–52]. After an optical excitation of the cavity, the laser power is turned off and the subsequent power decay of the radiation is observed by a photodetector. As usually, the analyzed gas sample is placed in the cavity.

6. Photoacoustic spectroscopy

In the photoacoustic spectroscopy, a signal occurs due to conversion of a light energy into an acoustic wave [53]. The light beam is modulated as it is shown in Fig. 12. When it is absorbed in the medium, the gas temperature is periodically changed and the acoustic wave with modulation frequency is observed. The wave is detected by using a sensitive microphone.

Among the so-called *in-situ* methods, PAS belongs to the most popular. The photoacoustic signal depends on the absorber concentration in the investigated sample. The signal amplitude at the microphone's output is given by

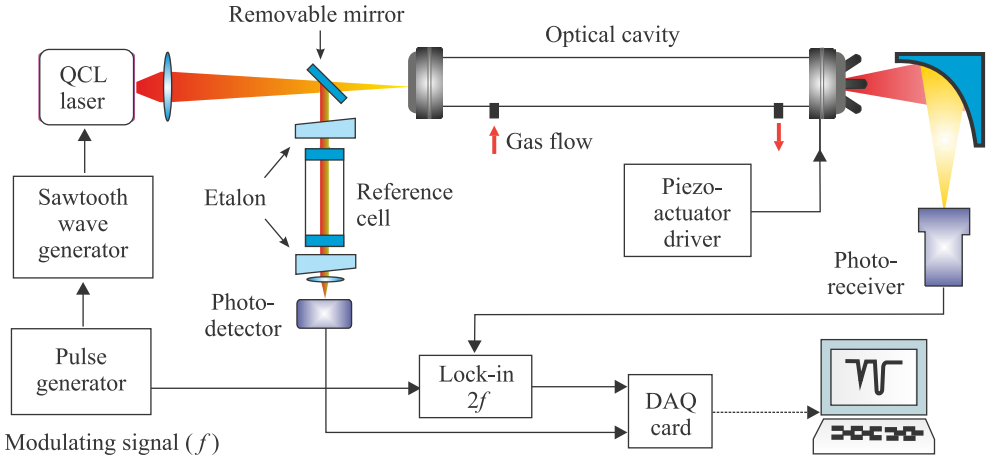

Fig. 11. Operation principle of ICOS method.

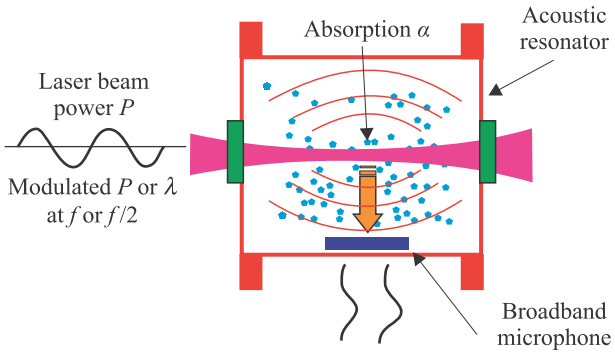

Fig. 12. Idea of photoacoustic spectroscopy.

$$A(T,\lambda) \propto P_o N \alpha(T,\lambda) L \frac{m}{vV} \eta \,, \tag{16}$$

where P_o denotes the average laser power, m is the modulation coefficient of radiation, v is the frequency of modulation, V is the gas volume, and η is the microphone efficiency.

The main disadvantage of PAS sensors is their sensitivity to mechanical and acoustic vibrations. In order to increase immunity from these noises, various acoustic resonators are applied. Effectiveness of these solutions is limited when the conventional microphones of a flat frequency response are used.

The sensitivity of PAS was recently increased many times due to the use of resonance quartz microphones [54–56]. Low-frequency quartz forks (QTF) with the resonance at 32768 Hz in vacuum have been applied [Fig. 13(a)] [57]. Only the symmetric vibration of a QTF is piezoelectrically active. The excitation beam passes through the gap between the QTF prongs for efficient excitation of this vibration. Acoustically, a QTF is a quadrupole which results in an excellent environmental noise immunity. Sound waves from distant acoustic sources tend to move the QTF prongs in the same direction, thus resulting in no electrical response.

So-called quartz-enhanced photoacoustic spectroscopy (QEPAS) is characterized by a simple design, immunity from environmental acoustic noise, applicability over a wide range of pressures including atmospheric pressure and the capability to analyse small gas samples, down to 1 mm^3 in volume. A setup of QEPAS based trace gas detection is shown in Fig. 13(b). In the setup, the measurements are usually made with a wavelength modulation approach and $2f_0$ detection method which suppresses the background originating from spectrally non-selective absorbers (such as resonator walls, QTF electrodes, and gas cell elements). A lock-in amplifier is used to demodulate the QTF response. Spectral data can be acquired if a laser wavelength is scanned. In order to increase the effective interaction length between the radiation-induced sound and the QTF, an acoustic gas-filled resonator can be added similarly to the traditional PAS approach.

QEPAS provides opportunity to construct the sensors of the best detection sensitivity. The detection sensitivity of absorption by QEPAS reaches α_L ~5×10^{-8}cm^{-1}, for the laser power of 1 W.

7. Conclusions

Although all the spectroscopic methods, which are mentioned above, are characterized by large sensitivity, each of them is affected by limitations. CRDS is very useful in the radiation spectral range where the most sensitive photodetectors (photomultipliers) are available: from UV to 1.7 μm. The problems occur for longer wavelengths due to relatively low photodetection responsivity (highly sensitive photoreceiver with HgCdTe photodiodes developed by Vigo System S.A., Poland would find here a good application). Low-power laser radiation causes additional detection difficulties due to signal quenching when passing through the highly reflecting mirrors of the resonator. Here, PAS or QEPAS methods might be the solution, however, in order to deliver their high sensitivity a laser source of power at the

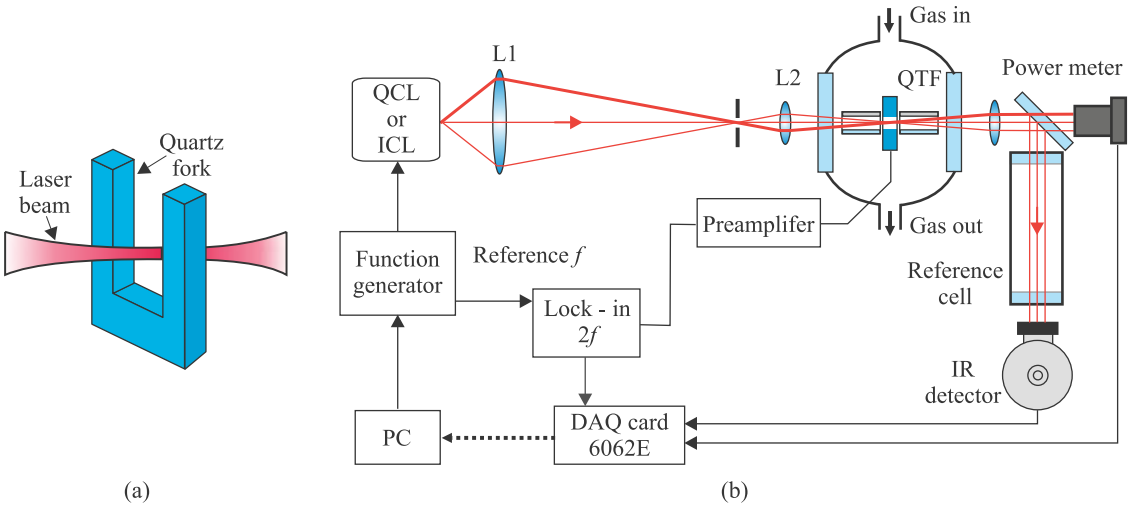

Fig. 13. Idea of quartz forks (QTF) based absorption detection module (a) and merits of QEPAS based trace gas detection (b).

Table 5. Some biomarkers in human breath, their detection methods and achieved sensitivity.

Biomarker	Wavelength range (μm)	Spectroscopic technique	Detected concentration
Acetaldehyde (CH_3COH)	5.79	TDLAS	80 ppb [60]
Acetone ($OC(CH_3)_2$)	0.266	CRDS	0.2 ppm [61–63]
Ammonia (NH_3)	9–10.7	PAS	100 ppm [64]
	11.0	TDLAS	1 ppm [65]
	10.0	TDLAS	50 ppb [66]
	10.0	TDLAS	3 ppb [67]
	10.3	TDLAS	5 ppb [68]
	1.5	OFC-CEAS	4 ppm [69]
	~10.6 μm	QEPAS	<10 ppb [70]
Carbon dioxide and C-isotope [CO_2 & $^{13}CO_2/^{12}CO_2$]	4.23	PAS	7 ppb [71]
CO_2	1.6	CRDS	3 ppm [72]
	1.59	TDLAS/WM	100 ppm [73]
	4.9	TDLAS	0.5 ppm [69]
Carbon monoxide (CO)	1.6	OFC-CEAS	900 ppb [69]
	4.6	TDLAS	0.5 ppm [69]
Carbonyl sulphide (OCS)	4.86	TDLAS	1.2 ppb [74]
	4.86	TDLAS	30 ppb [75]
	4.9	CALOS	438 ppt [76]
D/H isotopic ratio (D_2O/H_2O)	3.50–3.65	TDLAS	55.2% ±1.8% body water [77]
Ethane (C_2H_6)	3.4	OA-ICOS	0.12 ppb [78]
	3.4	TDLAS	0.1 ppb [79]
	3.3	CALOS	270 ppt [50]
	3.0	CALOS	100 ppt [80]
	2.6–4.0	CALOS	500 ppt [81]
	3.4	TDLAS	0–12 ppb [82]
	3.4	TDLAS/WM	70 ppt [83]
Ethylene (C_2H_4)	10.5	PAS	– [84]
	9.2–10.8	PAS	– [85]
Formaldehyde (CH_2O)	3.53	ICOS	150 ppb [86]
	3.53	TDLAS	320 ppt [87]
	3.53	CALOS	2 ppb [88]
	3.53	PAS	3 ppb [89]
	3.53	QEPAS	0.6 ppm [90]
	3.53	TDLAS	77 ppt [91]
	3.53	TDLAS	1.2 ppm [92]
Methane (CH_4)	3.35	TDLAS	0.5 ppm [68]
Methylamine (CH_3NH_2)	1.51–1.53	CRDS	2.3 ppm [93]
Dimethylamine ($(CH_3)_2NH_3$)	1.51–1.53	CRDS	10 ppm [67]
Nitric Oxide (NO)	5.2	ICOS	1 ppb [94]
	5.2	TDLAS	2 ppb [95]
	5.2	TDLAS	3 ppb [96]
	5.2	CEAS	16 ppb [44]
	5.2	CRDS	0.7 ppb [97]
	5.2	TDLAS	1.5 ppb [98]
	5.2	TDLAS	2 ppb [99]
	5.2	ICOS	400 ppt [71]
^{14}NO and ^{15}NO	5.0	CALOS	7 ppt [100]

level of tens of milliwatts is required. As far as MPS is concerned, although its sensitivity is limited, it can be used in the cases when neither high power semiconductor lasers nor sensitive photodetectors are available. The intensity of the laser beam which passes through the multi-pass absorption cell is sufficient enough to be detected by common IR photodetectors. As one can see, the spectroscopic techniques complete each other.

An increase in sensitivity of the optical methods by several orders of magnitude is expected when the novel frequency standard as the optical frequency comb (OFC) will be applied. It might be used for control and stabilization of laser frequency as well as for very precise readout of molecular spectra. The precision, which is required by these measurements, can be achieved with single mode tuneable diode lasers or with QCLs which have appeared recently on the market. Their power reaches tens of milliwatts. These lasers are still expensive sources of radiation. However, analysing the progress in optoelectronic technology one can expect a significant reduction of their prices within the forthcoming years [58].

In conclusion, in the paper, the optical methods of detection of various biomarkers occurring in human breath were performed. Selected biomarkers and their spectroscopic methods of detection are listed in Table 5. These techniques provide opportunity to construct fully optoelectronic sensors applying contemporary laser spectroscopy techniques. The methods can be applied for *in situ* breath analysis research. It can also be used for no-direct investigation of air samples from patients with the use of recently developed collectors [59]. The collectors consist of the fibres covered by layers of polymers which can adsorb certain biomarkers. The compounds collected by fibres from large air volume can be desorbed in small volume sensors. In this way the marker concentration can be increased and an additional growth in detection sensitivity can be achieved.

These investigations are of a great importance for development of hi-tech tasks as well as for health and security protection. The obtained results will allow us to construct breath analysis systems for both medical offices and screening. The development of such absorption spectroscopy apparatus with semiconductor lasers can provide certain advantages not only for medical enterprises. It will also stimulate the design and performance of optoelectronic sensors of other various dangerous compounds.

References

1. "Specialized analysers for NO detection in breath are available on medical instrument market", www.shelfscientific. com.
2. A. Michalski, *Metrology in Medicine – Selected Problems*, Military University of Technology Publishing Office, Warsaw, 2011.
3. L. Pauling, A.B. Robinson, R. Teranishi, and P. Cary, "Quantitative analysis of urine vapour and breath by gas-liquid partition chromatography", *P. Natl. Acad. Sci. USA* **68**, 2374–2384 (1971).
4. H. O'Neill, S.M. Gordon, M. O'Neill, R.D. Gibbons, and J.P. Szidon, "A computerized classification technique for screening for the presence of breath biomarkers in lung cancer", *Clin. Chem.* **34**, 1613–1618 (1988).
5. C. Wang, and P. Sahay, "Breath analysis using laser spectroscopic techniques: breath biomarkers, spectral fingerprints, and detection limits", *Sensors* **9**, 8230–8262 (2009).
6. T. Kondo, T. Mitsui, M. Kitagawa, and Y. Nakae, "Association of fasting breath nitrous oxide concentration with gastric juice nitrate and nitrite concentrations and helicobacter pylori infection", *Digest. Dis. Sci.* **45**, 2054–2057 (2000).
7. R.A. Dweik, D. Laskowski, H.M. Abu-Soud, F.T. Kaneko, R. Hutte, D.J. Stuehr, and S.C. Erzurum, "Nitric oxide synthesis in the lung, regulation by oxygen through a kinetic mechanism", *J. Clin. Invest.* **101**, 660–666 (1998).
8. B. Enderby, D. Smith, W. Carroll, and W. Lenney, "Hydrogen cyanide as a biomarker for Pseudomonas aeruginosa in the breath of children with cystic fibrosis", *Pediatr. Pulm.* **44**, 142–147 (2009).
9. Z. Witkiewicz, *Principles of Chromatography*, Scientific-Technical Publishers (WNT), Warsaw, 2000. (in Polish)
10. W. Mueller, J. Schubert, A. Benzing, and K. Geiger, "Method for analysis of exhaled air by microwave energy desorption coupled with gas chromatography-flame ionization detection-mass spectrometry", *J. Chromatogr.* **B716**, 27–38 (1998).
11. X. Chen, F. Xu, Y. Wang, Y. Pan, D. Lu, and P. Wang, "A study of the volatile organic compounds exhaled by lung cancer cells in vitro for breath diagnosis", *Cancer* **110**, 835–844 (2007).
12. A. Ulanowska, T. Ligor, M. Michel, and B. Buszewski, "Hyphenated and unconventional methods for searching volatile cancer biomarkers", *Ecol. Chem. En.* **17**, 9–23 (2010).
13. http://www.chromacademy.com/resolver/nov2010/fig-jpg
14. http://sift-ms.net/user/cimage/SiftMsColourpng
15. T. Pustelny, *Physical and Technical Aspects of Optoelectronic Sensors*, Silesian University of Technology Publishing Office, 2005.
16. http://www.tms.org/pubs/journals/JOM/ 0010/Ivanov/fig4.gif
17. http://www.nature.com/nmat/journal/v2/n1/fig_tab/nmat768_F4.html
18. A. Bratkowski, A. Korcala, Z. Łukasik, P. Borowski, and W. Bala, "Novel gas sensor based on porous silicon measured by photovoltage, photoluminescence, and admittance spectroscopy", *Opto-Electron. Rev.* **13**, 35–38 (2005).
19. R. Maniewski, A. Liebert, M. Kacprzak, and A. Zbieć, "Selected application of near-infrared optical methods in medical diagnosis", *Opto-Electron. Rev.* **12**, 255–262 (2004).
20. J. Puton, K. Jasek, B. Siodłowski, A. Knap, and K. Wiśniewski, "Optimization of a pulsed IR source for NDIR gas analysis", *Opto-Electron. Rev.* **10**, 97–103 (2002).
21. M. Walczak, "Operant conditioning of dogs for detection of odour markers of cancer diseases", *PhD Dissertation*, Institute of Genetics and Animal Breeding of the Polish Academy of Sciences, Warsaw, Poland, 2009. (in Polish)
22. P. Kowalczyk, *Physics of Molecules*, Polish Scientific Publishers (PWN), Warsaw, 2000. (in Polish)
23. M.F. Merienne, A. Jenouvrier, and B. Coquart, "The NO_2 absorption spectrum. I: absorption cross-sections at ambient temperature in the 300-500 nm region", *J. Atmos. Chem.* **20**, 281–297 (1995).

24. M.I. Mazurenka, B.I. Fawcett, J.M.F. Elks, D.E. Shallcross, and A.J. Orr-Ewing, "410-nm diode laser cavity ring-down spectroscopy for trace detection of NO_2", *Chem. Phys. Lett.* **367**, 1–9 (2003).
25. J. Wojtas, A. Czyżewski, T. Stacewicz, and Z. Bielecki, "Detection of NO_2 using cavity enhanced methods", *Opt. Appl.* **36**, 461–467 (2006).
26. K. Holc, Z. Bielecki, J. Wojtas, P. Perlin, J. Goss, A. Czyżewski, P. Magryta, and T. Stacewicz, "Blue tunable laser diodes for trace matter detection", Opt. Appl. **40,** 641–651 (2010).
27. T. Stacewicz, J. Wojtas, Z. Bielecki, M. Nowakowski, J. Mikołajczyk, R. Mędrzycki, and B. Rutecka, "Cavity Ring Down Spectroscopy: detection of trace amounts of matter", *Opto-Electron*. Rev. **20**, (2012). (in press)
28. http://www.cfa.harvard.edu/HITRAN/
29. J. Wojtas, J. Mikołajczyk, M. Nowakowski, B. Rutecka, R. Mędrzycki, and Z. Bielecki, "Appling CEAS method to UV, VIS, and IR spectroscopy sensors", *B. Pol. Acad. Sci-Te.* **59**, No. 4 (brak stron) (2011).
30. http://badc.nerc.ac.uk/data/esa-wv
31. http://www.cfa.harvard.edu/HITRAN/
32. http://www.teledyne-ai.com/pdf/lga-3500.pdf
33. J.M. Chalmers, *Mid-infrared Spectroscopy. Spectroscopy in Process Analysis*, CRC Press LLC, 117, 1999.
34. http://www.ipm.fraunhofer.de
35. A. O'Keefe, and D.A.G. Deacon, "Cavity ring-down optical spectrometer for absorption measurements using pulsed laser sources", *Rev. Sci. Instrum.* **59**, 2544–2551 (1988).
36. K.W. Busch and M.A. Busch, *Cavity-Ringdown Spectroscopy*, *an Ultratrace-Absorption Measurement Technique*, ACS Symposium Series, American Chemical Society, Washington DC, 1999.
37. G. Berden, and R. Engeln, *Cavity Ring-Down Spectroscopy: Techniques and Applications*, Wiley-Blackwell, 2009.
38. Z. Bielecki and T. Stacewicz, *Optoelectronic Sensor of Nitrogen Dioxide*, *Analysis and Construction Requirements*, Military University of Technology Publishing Office, Warsaw, 2011. (in Polish)
39. D. Romanini, A.A. Kachanov, N. Sadeghi, and F. Stoeckel, "CW-cavity ring down spectroscopy", *Chem. Phys. Lett.* **264**, 316–322 (1997).
40. G. Berden, R. Peeters, and G. Meijer, "Cavity ring-down spectroscopy: Experimental schemes and applications", *Int. Rev. Phys. Chem.* **19**, 565–607 (2000).
41. J. Ye, L.S. Ma, and J.L. Hall, "Ultrastable optical frequency reference at 064 μm using a C2HD molecular overtone transition", *IEEE T. Instrument. Meas.* **46**, 178–182 (1997).
42. R. Engeln, G. Berden, R. Peeters, and G. Meier, "Cavity enhanced absorption and cavity enhanced magnetic rotation spectroscopy", *Rev. Sci. Instrum.* **69**, 3763–3769 (1998).
43. J.D. Ayers, R.L. Apodaca, W.R. Simpson, and D.S. Baer, "Off-axis cavity ring-down spectroscopy: application to atmospheric nitrate radical detection", *Appl. Opt.* **44**, 7239–7242 (2005).
44. L. Menzel, A.A. Kosterev, R.F. Curl, F.K. Tittel, C. Gmachl, F. Capasso, D.L. Sivco, J.N. Baillargeon, A.L. Hutchinson, A.Y. Cho, and W. Urban, "Spectroscopic detection of biological NO with a quantum cascade laser", *Appl. Phys.* **B72**, 859–863 (2001).
45. J.M. Herbelin, J.A. McKay, M.A. Kwok, R.H. Uenten, D.S. Urevig, D.J. Spencer, and D.J. Benard, "Sensitive measurement of photon lifetime and true reflectances in an optical cavity by a phase-shift method", *Appl. Opt.* **19**, 144–147 (1980).
46. F.K. Tittel, Yu. Bakhirkin, A.A. Kosterev, G. Wysocki, and S. So & R.F. Curl, "Recent advances of quantum and interband cascade laser based gas sensor technology", www.lancs.ac.uk/depts/spc/conf/miomd-7/Tittel.ppt
47. V. Spagnolo, R. Lewicki, L. Dong, and F. K. Tittel, "Quantum-cascade-laser-based optoacoustic detection for breath sensor applications", *IEEE* **978**, 332–335 (2011).
48. A. O'Keefe, "Integrated cavity output analysis of ultra-weak absorption", Chem. Phys. Lett. **293**, 331–336 (1998).
49. A. O'Keefe, J.J. Scherer, and J.B. Paul, "CW integrated cavity output spectroscopy", Chem. Phys. Lett. **307**, 343–349 (1999).
50. H. Dahnke, D. Kleine, C. Urban, P. Hering, and M. Murtz, "Isotopic ratio measurement of methane in ambient air using mid-infrared cavity leak-out spectroscopy", *Appl. Phys. B-Lasers O*. **72**, 121–125 (2001).
51. D. Halmer, S. Thelen, P. Hering, and M. Mürtz, "Online monitoring of ethane traces in exhaled breath with a difference frequency generation spectrometer", *Appl. Phys. B-Lasers O*. **85**, 437–443 (2006).
52. D. Halmer, G. von Basum, P. Hering, and M. Murtz, "Mid-infrared cavity leak-out spectroscopy for ultrasensitive detection of carbonyl sulphide", *Opt. Lett.* **30**, 2314–2316 (2005).
53. T. Starecki, *Selected Aspects of Photoacoustic Instruments Optimization*, BTC, Legionowo, 2009.
54. A.A. Kosterev, Y.A. Bakhirkin, R.F. Curl, and F.K. Tittel, "Quartz-enhanced photoacoustic spectroscopy", *Opt. Lett.* **27**, 1902–1904 (2002).
55. R.F. Curl and F.K. Tittel, "Tunable infrared laser spectroscopy", *Annu. Rep. Prog. Chem. Sect.* **C98**, 217–270 (2002).
56. F.K. Tittel, D. Richter, and A. Fried, "Mid-infrared laser applications in spectroscopy", *Springer. Topics Appl. Phys*. **89**, 445–510 (2003).
57. A. Kosterev, F.K. Tittel, D. Serebryakov, A. Malinovsky, and A. Morozov, "Applications of quartz tuning fork in spectroscopic gas sensing", *Rev. Sci. Instrum.* **76**, 043105 (2005).
58. M. Bugajski, K. Kosiel, A. Szerling, J. Kubacka-Traczyk, I. Sankowska, P. Karbownik, A. Trajnerowicz, E. Pruszyńska Karbownik, K. Pierściński, and D. Pierścińska, "GaAs/AlGaAs (9.4 μm) quantum cascade lasers operating at 260 K", *B. Pol. Acad. Sci-Te.* **58**, 471–476 (2010).
59. http://echozycia.ddsoft.pl/Files/file/%C5%81owcy%20oddech%C3%B3w.pdf
60. P.C. Kamat, C.B. Roller, K. Namjou, J.D. Jeffers, A. Faramarzalian, R. Salas, and P.J. McCann, "Measurement of acetaldehyde in exhaled breath using a laser absorption spectrometer", *Appl. Opt.* **46**, 3969–3975 (2007).
61. C. Wang, and A. Mbi, "A new acetone detection device using cavity ringdown spectroscopy at 266 nm: evaluation of the instrument performance using acetone sample solutions", *Meas. Sci. Technol.* **18**, 2731–2741 (2007).
62. C. Wang, A. Mbi, and M. Shepherd, "A study on breath acetone in diabetic patients using a cavity ring-down breath analyzer: Exploring correlations of breath acetone with blood glucose and glycohemoglobin A1C", *IEEE Sens*. **10**, 54–63 (2010).
63. C. Wang, and A.B. Surampudi, "An acetone breath analyzer using cavity ring-down spectroscopy: an initial test with hu-

man subjects under various situations", *Meas. Sci. Technol.* **19**, 105604–105614 (2008).
64. L.R. Narasimhan, W. Goodman, and C.K.N. Patel, "Correlation of breath ammonia with blood urea nitrogen and creatinine during hemodialysis", *P. Natl. Acad. Sci. USA* **98**, 4617–4621 (2001).
65. U. Lachish, S. Rotter, E. Adler, and U. El-Hanany, "Tunable diode laser based spectroscopic system for ammonia detection in human respiration", *Rev. Sci. Instrum.* **58**, 923–927 (1987).
66. J. Manne, O. Sukhorukov, W. Jager, and J. Tulip, "Pulsed quantum cascade laser-based cavity ring-down spectroscopy for ammonia detection in breath", *Appl. Opt.* **45**, 9230–9237 (2006).
67. J. Manne, W. Jager, and J. Tulip, "Sensitive detection of ammonia and ethylene with a pulsed quantum cascade laser using intra and interpulse spectroscopic techniques", *Appl. Phys. B-Lasers O.* **94**, 337–344 (2009).
68. K.L. Moskalenko, A.I. Nadezhdinskii, and I.A. Adamovskaya, "Human breath trace gas content study by tunable diode laser spectroscopy technique", *Infrared Phys. Techn.* **37**, 181–192 (1996).
69. M.J. Thorpe, D. Balslev-Clausen, M.S. Kirchner, and J. Ye, "Cavity-enhanced optical frequency comb spectroscopy: application to human breath analysis", *Opt. Express* **16,** 2387–2397 (2008).
70. R. Lewicki, A.A. Kosterev, Y.A. Bakhirkin, D.M. Thomazy, J. Doty, L. Dong, and F.K. Tittel, "Real time ammonia detection in exhaled human breath with a quantum cascade laser based sensor", *IEEE* **978**, 1–2 (2009).
71. M.M.J.W. Van Herpen, A.K.Y. Ngai, S.E. Bisson, J.H.P. Hackstein, E.J. Woltering, and F.J.M. Harren, "Optical parametric oscillator-based photoacoustic detection of CO2 at 4.23 μm allows real-time monitoring of the respiration of small insects", *Appl. Phys. B-Lasers O.* **82**, 665–669 (2006).
72. E.R. Crosson, K.N. Ricci, B.A. Richman, F.C. Chilese, T.G. Owano, R.A. Provencal, M.W. Todd, J. Glasser, A.A. Kachanow, B.A. Paldus, T.G. Spence, and R.N. Zare, "Stable isotope ratios using cavity ring-down spectroscopy: determination of $^{13}C/^{12}C$ for carbon dioxide in human breath", *Anal. Chem.* **74**, 2003–2007 (2002).
73. V. Weldon, J. O'Gorman, P. Phelan, J. Hegarty, and T. Tanbun-Ek, "H_2S and CO_2 gas sensing using DFB laser diodes emitting at 57 μm", *Sens. Actuat.* **B29**, 101–107 (1995).
74. G. Wysocki, M. McCurdy, S. So, D. Weidmann, C. Roller, R.F. Curl, and F.K. Tittel, "Pulsed quantum-cascade laser-based sensor for trace-gas detection of carbonyl sulphide", *Appl. Opt.* **43**, 6040–6046 (2004).
75. Ch. Roller, A.A. Kosterev, F.K. Tittel, K. Uehara, C. Gmachl, and D.L. Sivco, "Carbonyl sulfide detection with a thermoelectrically cooled midinfrared quantum cascade laser", *Opt. Lett.* **28**, 2052–2054 (2003).
76. M.R. McCurdy, Y. Bakhirkin, G. Wysocki, and F.K. Tittel, "Performance of an exhaled nitric oxide and carbon dioxide sensor using quantum cascade laser-based integrated cavity output spectroscopy", *J. Biomed. Opt.* **12**, 034034:1–034034:9 (2007).
77. R. Bartlome, and M.W. Sigrist, "Laser based human breath analysis: D/H isotope ratio increases following heavy water intake", *Opt. Lett.* **34**, 866–868 (2009).
78. K.R. Parameswaran, D.I. Rosen, M.G. Allen, A.M. Ganz, and T.H. Risby, "Off-axis integrated cavity output spectroscopy with a mid-infrared interband cascade laser for real-time breath ethane measurements", *Appl. Opt.* **48**, B73–B79 (2009).
79. K.D. Skeldon, L.C. McMillan, C.A. Wyse, S.D. Monk, G. Gibson, C. Patterson,; T. France, C. Longbottom, and M.J. Padgett, "Application of laser spectroscopy for measurement of exhaled ethane in patients with lung cancer", *Respir. Med.* **100**, 300–306 (2006).
80. H. Dahnke, D. Kleine, C. Urban, P. Hering, and M. Murtz, "Isotopic ratio measurement of methane in ambient air using mid-infrared cavity leak-out spectroscopy", *Appl. Phys. B-Lasers O.* **72**, 121–125 (2001).
81. G. von Basum, D. Halmer, P. Hering, M. Murtz, S. Schiller, F. Mueller, A. Popp, and F. Kuehnemann, "Parts per trillion sensitivity for ethane in air with an optical parametric oscillator cavity leak-out spectrometer", *Opt. Lett.* **29**, 797–799 (2004).
82. C.S. Patterson, L.C. McMillan, K. Stevenson, K. Radhakrishnan, P.G. Shiels, M.J. Padgett, and K.D. Skeldon, "Dynamic study of oxidative stress in renal dialysis patients based on breath ethane measured by optical spectroscopy", *J. Breath Res.* **1**, 026005:1–026005:8 (2007).
83. K.D. Skeldon, C. Patterson, C.A. Wyse, G.M. Gibson, M.J. Padgett, C. Longbottom, and L.C McMillan, "The potential offered by real-time, high-sensitivity monitoring of ethane in breath and some pilot studies using optical spectroscopy", *J. Opt. A-Pure Appl. Op.* **7**, S376–S384 (2005).
84. A. Puiu, G. Giubileo, and C. Bangrazi, "Laser sensors for trace gases in human breath", *Int. J. Environ. A. Ch.* **85**, 1001–1012 (2005).
85. D.C. Dumitras, D.C. Dutu, C. Matei, A.M. Magureanu, M. Petrus, C. Popa, and V. Patachia, "Measurements of ethylene concentration by laser photoacoustic techniques with applications at breath analysis", *Rom. Rep. Phys.* **60**, 593–602 (2008).
86. J.H. Miller, Y.A. Bakhirkin, T. Ajtai, F.K. Tittel, C.J. Hill, and R.Q. Yang, "Detection of formaldehyde using off-axis integrated cavity output spectroscopy with an interband cascade laser", *Appl. Phys. – Laser O.* **85**, 391–396 (2006).
87. D. Rehle, D. Leleux, M. Erdelyi, F. Tittel, M. Fraser, and S. Friedfeld, "Ambient formaldehyde detection with a laser spectrometer based on difference-frequency generation in PPLN", *Appl. Phys. B- Laser O.* **72**, 947–952 (2001).
88. H. Dahnke, G. von Basum, K. Kleinermanns, P. Hering, and M. Murtz, "Rapid formaldehyde monitoring in ambient air by means of mid-infrared cavity leak-out spectroscopy", *Appl. Phys. B-Lasers O.* **75**, 311–316 (2002).
89. M. Angelmahr, A. Miklos, and P. Hess, "Photoacoustic spectroscopy of formaldehyde with tunable laser radiation at the parts per billion level", *Appl. Phys. B-Lasers O.* **85**, 285–288 (2006).
90. M. Horstjann, Y.A. Bakhirkin, A.A. Kosterev, R.F. Curl, F.K. Tittel, C.M. Wong, C.J. Hill, and R.Q. Yang, "Formaldehyde sensor using interband cascade laser based quartz-enhanced photoacoustic spectroscopy", *Appl. Phys. B-Lasers O.* **79**, 799–803 (2004).
91. D. Richter, A. Fried, B.P. Wert, J.G. Walega, and F.K. Tittel, "Development of a tunable mid-IR difference frequency laser source for highly sensitive airborne trace gas detection", *Appl. Phys. B-Lasers O.* **75**, 281–288 (2002).
92. L. Ciaffoni, R. Grilli, G. Hancock, A.J. Orr-Ewing, R. Peverall, and *G.A.D.* Ritchie, "3.5-μm high-resolution gas

sensing employing a $LiNbO_3$ QPM-DFG waveguide module", *Appl. Phys. B-Lasers O.* **94**, 517–525 (2009).
93. D. Marinov, J.M. Rey, M.G. Muller, and M.W. Sigrist, "Spectroscopic investigation of methylated amines by a cavity-ringdown-based spectrometer", *Appl. Opt.* **46**, 3981–3986 (2007).
94. Y.A. Bakhirkin, A.A. Kosterev, C. Roller, R.F. Curl, and F.K. Tittel, "Mid-infrared quantum cascade laser based off-axis integrated cavity output spectroscopy for biogenic nitric oxide detection", *Appl. Opt.* **43**, 2257–2266 (2004).
95. K. Namjou, C.B. Roller, T.E. Reich, J.D. Jeffers, G.L. McMillen, P.J. McCann, and M.A. Camp, "Determination of exhaled nitric oxide distributions in a diverse sample population using tunable diode laser absorption spectroscopy", *Appl. Phys. B-Lasers O.,* **85**, 427–435 (2006).
96. L. Menzel, A.A. Kosterev, R.F. Curl, F.K. Tittel, C. Gmachl, F. Capasso, D.L. Sivco, J.N. Baillargeon, A.L. Hutchinson, A.Y. Cho, and W. Urban, "Spectroscopic detection of biological NO with a quantum cascade laser", *Appl. Phys. B-Lasers O.* **72**, 859–863 (2001).
97. A.A. Kosterev, A.L. Malinovsky, F.K. Tittel, C. Gmachl, F. Capasso, D.L. Sivco, J.N. Baillargeon, A.L. Hutchinson, and A.Y. Cho, "Cavity ringdown spectroscopic detection of nitric oxide with a continuous-wave quantum-cascade laser", *Appl. Opt.* **40**, 5522–5529 (2001).
98. C. Roller, K. Namjou, J.D. Jeffers, M. Camp, A. Mock, P.J. McCann, and J. Grego, "Nitric oxide breath testing by tunable-diode laser absorption spectroscopy: application in monitoring respiratory inflammation", *Appl. Opt.* **41**, 6018–6029 (2002).
99. K. Namjou, C.B. Roller, and G. McMillen, "Breath analysis using mid infrared tunable laser spectroscopy", *Proc. 6th Ann. IEEE Conf. on Sensors*, Atlanta, GA, USA, 1337–1340 (2007).
100. K. Heinrich, T. Fritsch, P. Hering, and M. Murtz, "Infrared laser-spectroscopic analysis of ^{14}NO and ^{15}NO in human breath", *Appl. Phys. B-Lasers O.* **95**, 281–286 (2009).

